This is an open access article published under a Creative Commons Attribution (CC-BY) License, which permits unrestricted use, distribution and reproduction in any medium, provided the author and source are cited.

ACS AUTHORCHOICE

ACS APPLIED MATERIALS & INTERFACES

www.acsami.org

Research Article

Green Conducting Cellulose Yarns for Machine-Sewn Electronic Textiles

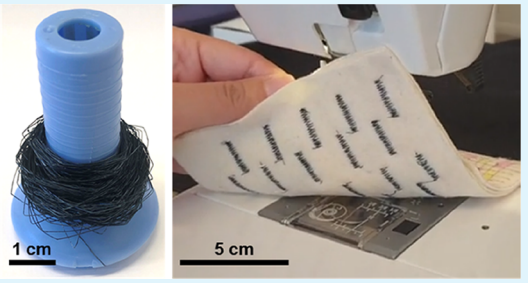
Sozan Darabi, Michael Hummel, Sami Rantasalo, Marja Rissanen, Ingrid Öberg Månsson, Haike Hilke, Byungil Hwang, Mikael Skrifvars, Mahiar M. Hamedi, Herbert Sixta, Anja Lund, and Christian Müller*

Cite This: *ACS Appl. Mater. Interfaces* 2020, 12, 56403−56412

Read Online

ACCESS | Metrics & More | Article Recommendations | Supporting Information

ABSTRACT: The emergence of "green" electronics is a response to the pressing global situation where conventional electronics contribute to resource depletion and a global build-up of waste. For wearable applications, green electronic textile (e-textile) materials present an opportunity to unobtrusively incorporate sensing, energy harvesting, and other functionality into the clothes we wear. Here, we demonstrate electrically conducting wood-based yarns produced by a roll-to-roll coating process with an ink based on the biocompatible polymer:polyelectrolyte complex poly(3,4-ethylenedioxythiophene):poly(styrene sulfonate) (PEDOT:PSS). The developed e-textile yarns display a, for cellulose yarns, record-high bulk conductivity of 36 Scm^{-1}, which could be further increased to 181 Scm^{-1} by adding silver nanowires. The PEDOT:PSS-coated yarn could be machine washed at least five times without loss in conductivity. We demonstrate the electrochemical functionality of the yarn through incorporation into organic electrochemical transistors (OECTs). Moreover, by using a household sewing machine, we have manufactured an out-of-plane thermoelectric textile device, which can produce 0.2 μW at a temperature gradient of 37 K.



KEYWORDS: *e-textile, conducting cellulose yarn, PEDOT:PSS, organic electrochemical transistor (OECT), organic thermoelectrics*

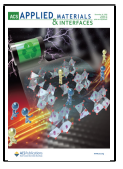
INTRODUCTION

Miniaturized electronic devices are increasingly present in our everyday lives. They are used in a wide range of applications including smart homes, active packaging, mini displays, and wearable or even implantable health monitoring, which typically rely on battery-powered miniature sensors connected to a wireless communication network. The expected lifetime of electronic devices can be very short, down to a few months, resulting in a massive and global buildup of electronic waste.[1] In addition, traditional electronics rely on scarce and, in some cases, toxic materials such as gallium arsenide, lead, cadmium, and indium.[2,3] Both, the exploitation of our natural resources and the management of waste need to be addressed to ensure a sustainable future for generations to come. This is a strong motivation for the development of "green" electronics, relying instead on nontoxic, renewable, and biodegradable organic precursors.[4] A variety of electronic devices on biobased substrates have been reported such as silk,[5] cellulose,[6] gelatin,[7] potato starch,[8] or DNA.[9] Furthermore, the conducting and semiconducting components can be realized with π-conjugated molecules commonly used as dyestuffs, e.g., indigo,[10] or with conjugated polymers including polyaniline, polypyrrole (PPy), and polythiophenes.[4]

Organic materials are inherently light-weight and flexible, and in combination with the fact that they are, in many cases, biocompatible (and even edible),[11] this makes them particularly attractive for applications where electronics are worn close to or directly on the body. The limited mechanical integrity of conjugated molecules can be overcome by blending them with an insulating material, resulting in conducting bulk materials, which can be molded into various shapes. For example, composites of cellulose with conjugated polymers and/or carbon nanoparticles can function as an active component in supercapacitors, batteries, light emitting diodes, solar cells, strain sensors, electrochemical transistors, and thermoelectric devices.[12−18] Further, cellulose, which stands out as it is the most abundant polymer in nature, can be used as a substrate material. Cellulose in the form of paper is widely explored as a substrate for flexible electronics, and several reviews on paper- and cellulose-based electronics are available.[6,15,19,20]

For wearable electronics, electronic textiles (e-textiles), with functionality fully integrated in the textile and its fibers, present an interesting opportunity to realize truly unobtrusive devices. There exist three basic routes to prepare e-textile fibers as follows:[21] (1) fiber spinning with conducting blends or

Received: August 26, 2020
Accepted: November 16, 2020
Published: December 7, 2020



Downloaded via CHUNG-ANG UNIV on January 13, 2021 at 05:58:59 (UTC).
See https://pubs.acs.org/sharingguidelines for options on how to legitimately share published articles.

© 2020 American Chemical Society

https://dx.doi.org/10.1021/acsami.0c15399
ACS Appl. Mater. Interfaces 2020, 12, 56403−56412

Table 1. Overview of the Electrical Conductivity (σ) of Previously Reported Cellulose Fibers and Representative Examples of Non-Cellulose Materials

material	conducting component	method of manufacture	σ (Scm^{-1})	ref.
cellulose	PEDOT:PSS	dip-coating, cotton yarn	15	25
	rGO[a]	dip-coating, cotton yarn	1	27
	MWNT/PPy	dip-coating/interfacial polymerization, cotton yarn	10	28
	PEDOT	oCVD[b], viscose fiber	14	26
	carbon black (50 wt %)	wet spinning, regenerated cellulose matrix	0.6	29
	MWNT (10 wt %)	wet spinning, regenerated cellulose matrix	0.002	30
	MWNT (10 wt %)	dry-jet wet spinning, regenerated cellulose matrix	31	22
	MWNT (3 wt %)	wet spinning, regenerated cellulose matrix	0.09	31
	MWNT (8 wt %)	wet spinning, regenerated cellulose matrix	1	31
	MWNT (5 wt %)	dry-jet wet spinning, regenerated cellulose matrix	0.0009	32
	MWNT (4 wt %)	dry-jet wet spinning, regenerated cellulose matrix	0.008	33
	PEDOT:PSS	dip-coating, regenerated cellulose yarn	36	this work
	PEDOT:PSS/Ag NW[c]	dip-coating, regenerated cellulose yarn	181	this work
non-cellulose	PEDOT:PSS	dip-coating, Spandex fabric	2	34
	PEDOT:PSS	dip-coating, silk threads	14	25
	PEDOT:PSS	R2R dip-coating, silk threads	70	35

[a]rGO = reduced graphene oxide [b]oCVD = oxidative chemical vapor deposition [c]Ag NW = silver nanowires

composites, (2) coating of cellulose yarns/fibers with conducting materials, and (3) polymerization of conducting polymers onto cellulose yarns/fibers. However, none of these routes have resulted in cellulose yarns with a high electrical conductivity and a high degree of wash and wear resistance. For example, route 1 has resulted in yarns with an electrical conductivity of up to 31 Scm^{-1} (Table 1 and Table S1), where Rahatekar et al. used dry-jet wet spinning to make cellulose composite fibers with an incorporation of 10 wt % multiwalled carbon nanotubes (MWNT).[22] The health risks related to carbon nanoparticles have been under investigation for some time, and carbon nanotubes were recently added to the SIN (Substitute It Now) list developed by ChemSec.[23,24] With this in mind, we opted to use the polymer:polyelectrolyte complex poly(3,4-ethylenedioxythiophene):poly(styrene sulfonate) (PEDOT:PSS), which is known to be biocompatible,[4] as our conducting component. A previous report from our group shows that cotton yarn can be dipcoated, i.e., route 2, with PEDOT:PSS to achieve a bulk conductivity of 15 Scm^{-1}.[25] Bashir et al. followed route 3 by depositing PEDOT on viscose fibers through oxidative chemical vapor deposition (oCVD) and obtained a conductivity of 14 Scm^{-1}.[26] For cellulose yarns to be an attractive and competitive e-textile component, their electrical conductivity needs to be increased further.

Cellulose-based textiles can be prepared from naturally occurring fibers, e.g., cotton and flax, or from regenerated cellulose using a variety of sources (wood, bamboo, hemp, and more). Cotton has long been a base fiber for apparel, as its fibers are both soft and hydrophilic ensuring comfort for the wearer. In addition, many textile-industry processes (yarn spinning, weaving, knitting, and dyeing) are developed and optimized for cotton fibers. However, cotton cultivation commonly results in the extensive use of pesticides, fertilizer, fresh water, and arable land.[36] Therefore, much effort is made to replace cotton with fibers made from regenerated cellulose whose raw material is wood. In fact, the development of innovative renewable forest products is identified by the United Nations as one of the key principles toward a sustainable development.[37] Regenerated cellulose fibers are still mainly produced *via* the viscose process. This process involves carbon disulfide, for cellulose derivatization, which is prone to form various toxic side products in the spinning plant. The only commercially relevant alternative is the Lyocell process using *N*-methylmorpholine *N*-oxide as a direct cellulose solvent.[38] This spinning technology requires high processing temperatures and stabilizers to avoid thermal runaway reactions.[39] An alternative method, aiming to be more cost-effective and more versatile in terms of feedstock, uses ionic liquids to dissolve the ligno-cellulosic material.[40,41] Regenerated cellulose yarns spun from ionic liquids have not yet been studied for use as e-textile materials.

Here, we present an electrically conducting yarn based on regenerated cellulose spun from an ionic liquid and coated with PEDOT:PSS, which is applied by a continuous roll-to-roll method. The coating process is based on our previously developed roll-to-roll method.[35] The resulting electrical conductivity of the yarn is 36 Scm^{-1}, which was further enhanced to 181 Scm^{-1} upon the addition of Ag nanowires. Our conducting yarn is resilient to repeated deformation and can be washed at least five times in a household washing machine without the loss of conductivity. Its mechanical stability in combination with the readily scalable coating process allowed us to use the yarn in a sewing machine to fabricate an energy harvesting thermoelectric textile.

EXPERIMENTAL SECTION

Materials. Regenerated cellulose yarns were spun according to the Ioncell process described elsewhere.[42] Enocell birch prehydrolysis kraft pulp (Stora Enso, Finland) was dissolved in 1,5-diazabicyclo[4.3.0]-non-5-enium acetate (13 wt % polymer concentration) and spun at 75 °C. A 400 hole spinneret (capillary diameter 100 μm; capillary length 20 μm) was used to yield a multifilament yarn. After washing and drying, each individual filament had a diameter of 11.7 ± 0.3 μm. PH1000 PEDOT:PSS aqueous dispersion (a 1.1−1.3 wt % solid content) was purchased from Heraeus. Ethylene glycol (EG) (Fisher Scientific) and dimethyl sulfoxide (DMSO) (VWR international) were used as received.

Ink Preparation and Coating. An amount of 5 vol % EG was added to the as-received PEDOT:PSS aqueous dispersion, followed by the removal of some water by heating at 50 °C for 47 h. This procedure has previously been found to increase the viscosity of the solution by 2 to 3 orders of magnitude, which in turn increases the ink take-up rate and final conductivity of the yarn.[35] Using a custom designed roll-to-roll setup, we continuously passed the yarn through a vessel containing the ink, at a speed of 0.23 m min^{-1}. Next, the yarn was dried with a heating

https://dx.doi.org/10.1021/acsami.0c15399
ACS Appl. Mater. Interfaces 2020, 12, 56403−56412

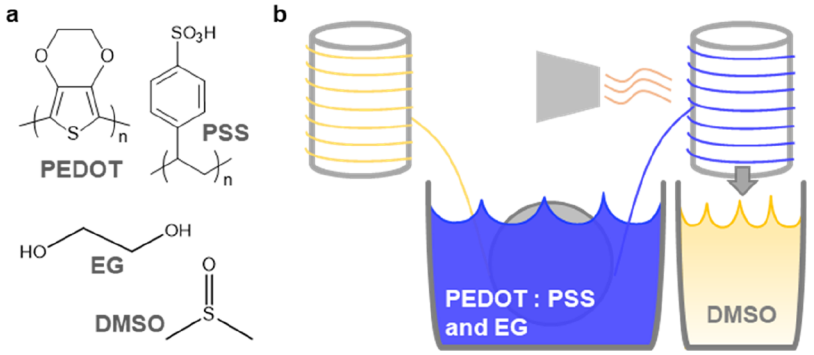


Figure 1. (a) Chemical structures of PEDOT:PSS, EG, and DMSO. (b) Schematic of the yarn-dyeing process: the pristine yarn travels through the dye bath and is then dried by a heating gun and collected. Afterward, the coated yarn is post-treated with DMSO.

gun at about ∼100 °C and collected onto a take-up roller. For post-treatment, the roll with the coated yarn was placed in a DMSO bath for 80 min and then dried again with a heat gun at ∼100 °C.

The PEDOT:PSS+Ag nanowire-coated cellulose yarns were produced by a batch process, where pieces of the cellulose yarn were dip-coated in an Ag nanowire solution (5 g L^{-1} in isopropyl alcohol, Sigma-Aldrich) according to the procedure reported by Hwang et al.[43] The average diameter and length of the Ag nanowires were 40 ± 5 nm and 35 ± 5 μm. The coated yarn was dried on a heating plate at 80−90 °C for a few seconds. The coating and drying process was repeated; however, the second drying was at 180 °C for 5 min. Finally, the Ag nanowire-coated yarn was twice dip-coated in a dispersion of PEDOT:PSS + 5 vol % EG and dried with a heating gun at ∼100 °C.

Mechanical Characterization. Tensile testing was performed on multifilament yarn samples using a Tinius Olsen H10KT dual-column testing machine equipped with fiber grips. A preload of 0.5 N was applied during the test, the gauge length was 40 mm, and the sample was drawn at 10 mm min^{-1} until break. The cross-sectional area of the yarns was estimated by comparing the linear density of neat and coated yarns, determined by measuring the weight of known lengths of yarn, and assuming a density of 1.5 g cm^{-3} for regenerated cellulose and 1 g cm^{-3} for PEDOT:PSS.

Electrical Characterization. The electrical resistivity of a spin-coated film of PEDOT:PSS (5% EG) was measured with a four-point probe setup from Jandel Engineering (cylindrical probe head, RM3000). To characterize the electrical resistance of coated yarns, samples were placed on a glass slide and colloidal silver paint (Agar Scientific) was applied to form contact points on the surface of PEDOT:PSS-coated yarns. In case of yarns with a composite coating of Ag nanowires and PEDOT:PSS, no silver paint was applied. The electrical resistance was measured in 2-point configuration, using a Keithley 2400 sourcemeter. To determine the contact resistance inherent to our 2-point measurements, we compared the resistance of segments with different lengths (Figure S1). Bending tests were performed using a custom-built Lego device in which the yarn was placed on a plastic film substrate (attached only at each end) and repeatedly bent to a radius of 4.3 mm. The yarn ends were coated with silver paint, and the electrical resistance of the yarn was measured after every 100 cycles, for a total of 1000 bending cycles. Fatigue testing was done in a dynamic mechanical tester DMA Q800 (TA Instruments) where a strain of 3% was applied for 6 s then released for 30 s. This was repeated for 101 cycles, and the electrical resistance was recorded *in situ* using a Keysight U1253B multimeter, which was connected to the yarn by crocodile clips attached to the silver paint-coated yarn ends. The Seebeck coefficient was measured using a SB1000 instrument together with a K2000 temperature controller (MMR Technologies). The experiment was carried out at 300 K with a thermal load of ∼2 K. The yarn sample, length ∼5 mm, was mounted onto a sample holder with silver paint, and a thin constantan wire was used as reference.

Optical Microscopy. A Carl Zeiss A1 optical microscope was used in bright field transmission mode to measure the diameter of the yarn.

Scanning Electron Microscopy (SEM). SEM images were obtained using a Leo Ultra 55 SEM with a secondary electron detector, at an acceleration voltage of 3 kV. The yarn samples were placed in liquid nitrogen and then immediately cut with a razor blade. The pristine sample was sputtered with palladium prior to microscopy analysis.

Laundering. Each specimen of the coated yarn was sewn onto a piece of multifiber adjacent test fabric (Testfabrics, Inc.) and washed up to 10 times in a domestic laundry machine (Bosch VarioPerfect, Serie 6) with 20 mL of a commercial detergent (Neutral) using wool wash program (30 °C, spin at 800 rpm). After washing, each multifiber test fabric (with segments of triacetate, cotton, polyamide, polyester, polyacrylic and viscose) was visually inspected for signs of release of the PEDOT:PSS coating, the coated yarn was visually inspected for a loss of coating, and the electrical resistance was characterized.

Organic Electrochemical Transistors. Yarn-based organic electrochemical transistor (OECT) devices were fabricated by attaching yarns to a plastic slide with tape. The PEDOT:PSS-coated yarn was used as the source-drain electrode, and a silver coated polyethylene terephthalate (PET) yarn (dtex 125/36/2 from Swicofil) was used as gate electrode. A single PEDOT:PSS-coated cellulose yarn was used for the source-drain electrode. The electrodes were positioned in parallel with a 2.5 mm separation. Nail varnish (Mavala International SA) was applied to act as fluidic barriers, preventing the electrolyte from wicking along the yarn to the electrical connections, leaving a 5 mm source-drain channel in contact with the electrolyte. Further, silver paste (Sigma Aldrich) was patterned onto the ends of the PEDOT:PSS-coated yarns to improve the connection to the clamp. An amount of 40 μL of phosphate-buffered saline (PBS, Sigma Aldrich) was added to bridge the source-drain and gate electrodes. $I-V$ characteristics, transfer characteristics, and ON/OFF switching were recorded for five individual devices using a Keithley 4200A parameter analyzer (Tektronix Inc., UK). For the $I-V$ characteristics, the source-drain potential (V_{sd}) was swept from 0 to −0.5 V while increasing the gate potential (V_g) from 0 to 0.7 V in steps of 0.1 V with a hold time of 30 s between each sweep, and the source-drain current (I_{sd}) response was recorded. The transfer characteristics were recorded by sweeping V_g between 0 and 0.8 V while recording I_{sd} at a fixed V_{sd} of −0.5 V, with a hold time of 15 s before each sweep. Lastly, the ON/OFF switching was recorded by measuring I_{sd} at a fixed V_{sd} of −0.5 V while holding the V_g at 0 and 0.8 V respectively, one complete cycle being 40 s.

Thermoelectric Device Manufacture. A Janome Easy Jeans 1800 sewing machine was used to sew a textile out-of-plane thermoelectric device, with a felted wool fabric (Wadmal, ∼1 mm thick, 3.2 g dm^{-2} from Harry Hedgren AB) as the insulating substrate. The conducting components were our coated cellulose yarn and a commercial silver-plated polyamide embroidery thread (HC12 from Madeira Garnfabrik). The conducting threads were transferred to the appropriate bobbins, and prior to sewing, the thread tension was adjusted to ensure that the conducting thread would completely penetrate the fabric so that it could be electrically connected on both sides of the fabric. A stretchable silver paste for conducting textile coatings (PE874, DuPont) was applied to offer electrical connections between the thermocouples of the textile device and was cured at 100 °C for 10 min.

https://dx.doi.org/10.1021/acsami.0c15399
ACS Appl. Mater. Interfaces 2020, 12, 56403−56412

Thermoelectric Device Characterization. The thermoelectric textile was placed on a variable temperature hot plate (HP60, Torrey Pines Scientific Inc). Surface-mounted K-type thermocouples (Omega Engineering) were placed on the top and bottom of the textile, to monitor the surface temperatures via a National Instruments cDAQ 9174 with an internal temperature reference. A cooling plate (Staychill) was placed on top of the thermoelectric textile, and thin sheets of Kapton (50 μm thickness) were placed on the top and bottom of the textile to prevent electrical short circuits. The generated voltage was recorded by a Keithley 2400 SMU, which also acted as a variable load by drawing current from the textile device.

RESULTS AND DISCUSSION

To manufacture our green electronic textiles, we aimed to use materials and processing methods that in addition to being eco-friendly are scalable and affordable, to ensure a potentially broad use for our developed materials.[44] The electrically conducting polymer:polyelectrolyte complex PEDOT:PSS (Figure 1a) is commercially available in the form of aqueous dispersions. As substrates, we selected regenerated cellulose fibers, dry-jet wet spun from an ionic liquid solution into an aqueous coagulation bath as previously reported,[40] and coated them, using a lab-scale continuous coating device, with an ink based on PEDOT:PSS (Figure 1b). The electrical conductivity of PEDOT:PSS materials is well studied, especially in the form of thin films, and it is known that the final conductivity can be improved by several orders of magnitude by post-treatments with polar solvents.[45] We chose a protocol that we had previously developed for silk yarns and dyed cellulose yarns with a thickened PEDOT:PSS ink to which we added 5 vol % ethylene glycol (EG), followed by a post treatment with dimethyl sulfoxide (DMSO).[35] We coated ~70 m of cellulose filament yarns with a continuous process (Figure 2a).

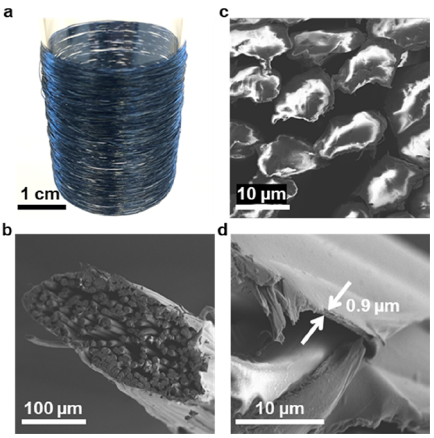


Figure 2. (a) Photograph of a roll of ~70 m of conducting cellulose yarn. SEM-images of (b) the cross-section of the coated yarn, (c) close-up of the cross-section, and (d) the coating layer covering the yarn perimeter with the thickness shown. No sputtering was done before imaging.

We also used a batch process to produce yarns coated with two layers of Ag nanowires before coating with PEDOT:PSS. The combination of Ag nanowires with PEDOT:PSS results in a washable conducting coating where the electric current is mainly carried by the silver, as was recently reported by our group.[43] This option offers a simple method for the manufacture of e-textiles that require highly conducting materials, which are suitable for the realization of electrical connectors or Joule heating elements. Instead, yarns produced without Ag nanowires can be used to construct electrochemical or thermoelectric devices.

It is common in e-textile literature to report the surface resistance and report this value in terms of $\Omega/\square$ or in Scm^{-1} based on an estimated thickness of the conducting layer (cf. Table S1). We argue that, for a fair comparison between fibers and yarns, it is relevant to instead characterize the "bulk" volume conductivity (σ_b), i.e., we calculate the cross-section area A of the conductor using the average thread diameter as observed by optical microscopy. In this approach, a large portion of the characterized volume is constituted of insulating cellulose and voids between filaments, and σ_b will be relatively low compared to the conductivity of the conducting component. The bulk conductivity σ_b is given by

$$\sigma_b = \frac{l}{A \times (R - R_c)} \quad (1)$$

where l is the sample section length, A is the cross-sectional area of the thread (diameter of 0.17−0.25 mm, determined with an optical microscope), R is the measured total resistance, and R_c is the contact resistance inherent to our 2-point measurement (Figure S1). Yarns coated with two layers of PEDOT:PSS displayed a bulk electrical conductivity of 36 Scm^{-1}, while yarns with a composite coating of Ag nanowires and PEDOT:PSS displayed a value of 181 Scm^{-1} (Table 2). Neat yarns had a linear density of 12.0 Tex (g per 1000 m), while yarns coated with two layers of PEDOT:PSS had 14.2 Tex, meaning that 16% of the weight of the coated yarn consisted of PEDOT:PSS. Comparison with the diameter obtained from optical microscopy indicates that the coating layer has a conductivity of about 514 S cm^{-1}. A spin-coated film of PEDOT:PSS (5% EG) had a similar conductivity of 840 S cm^{-1}. For the yarn with a composite coating of Ag nanowires and PEDOT:PSS, we instead obtain 29.1 Tex, indicating that the conducting coating constitutes 59% of the total weight.

To study the microstructure of coated yarns, we performed scanning electron microscopy (SEM) of cross-sections (Figure 2b−d and Figures S2 and S3). From the micrographs, we find that the coating has formed a submicrometer-thin continuous layer around the perimeter of the multifilament (Figure 2d). SEM imaging of a sample without a sputtered conducting layer indicates that the initially circular and smooth filaments (Figure S4) now have a thin coating layer, which is evidently electrically conducting, resulting in a lack of charging artefacts close to the

Table 2. Processing Parameters, Bulk Conductivity (σ_b) as Measured on n Samples, Young's Modulus (E), and Strain at Break (ε_{break}) as Measured on m Samples[a]

coating	no. of coating layers	post processing treatment	σ_b (Scm^{-1})	n	E (GPa)	ε_{break} (%)	m
PEDOT:PSS + EG	1	DMSO	24 ± 5	12	3.5 ± 0.1	13 ± 9	3
PEDOT:PSS + EG	2	DMSO	36 ± 10	18	3.6 ± 0.1	8 ± 2	3
Ag nanowires, then PEDOT:PSS + EG	2*		181 ± 71	4	n.m.	n.m.	n.m.

[a]n.m. = not measured. *Twice dip-coated with Ag nanowires and then twice with PEDOT:PSS + EG, batch processing.

https://dx.doi.org/10.1021/acsami.0c15399
ACS Appl. Mater. Interfaces 2020, 12, 56403−56412

filament surface (Figure 2c). The makeup of the coating layer was confirmed by energy-dispersive X-ray spectroscopy (EDX) to consist of PEDOT:PSS, as indicated by the presence of sulfur (Figure S5). Additional information regarding the PEDOT:PSS coating layer is shown in Figures S6 and S7.

We proceeded to evaluate the electromechanical stability of our conducting yarns. First, tensile tests were performed on yarns coated with one and two layers of PEDOT:PSS. The strain at break ε_{break} was 15% for the yarns with one layer of coating, whereas there is a decrease to $\varepsilon_{break} \approx 8\%$ after coating with two layers (Figure 3a and Table 2).

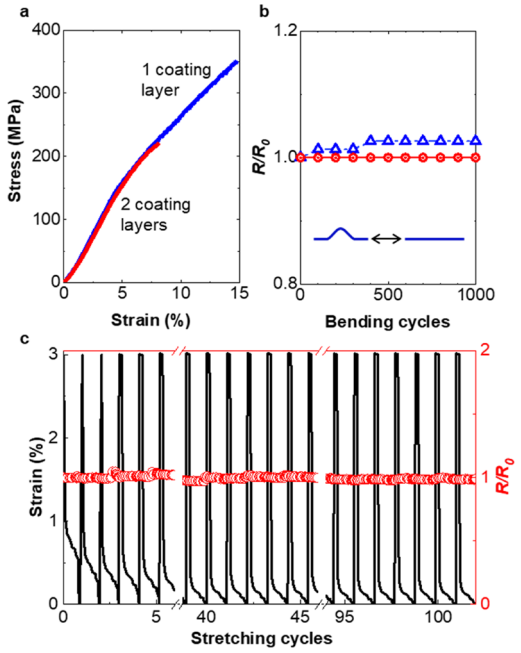


Figure 3. (a) Tensile test of conducting yarns with one (blue line) or two (red line) coating layers. (b) The ratio of measured electrical resistance (R) and initial electrical resistance (R_0) after up to 1000 cycles of bending with a bending radius of 4.3 mm for yarns coated with either one (blue open triangle) or two (red open circle) coating layers. (c) R/R_0 for the twice coated yarn (red open circles) measured *in situ* during 101 stretching cycles (strain rate 0.5 s^{-1}, grey lines) to 3% strain.

To further evaluate the mechanical resilience, we subjected the yarns to repeated bending by mounting it in a custom-built Lego device that repeatedly introduced a curvature with a 4.3 mm radius. We measured the electrical resistance of the yarn after every 100th bend cycle, and in total, the yarns were bent 1000 times. After evaluating yarns with either one or two coating layers in this setup, we found only a slight increase in R/R_0 (R_0 = the measured resistance prior to bending) for the once-coated yarn and no increase for the twice coated yarn (Figure 3b). We proceeded to subject the twice-coated yarn to cyclic tensile strain: the yarn was stretched to 3% at a draw rate of 0.019 μm s^{-1} and then released for 30 s. This was repeated 101 times, and the electrical resistance was recorded *in situ*. The results show no significant change in resistance during the 101 cycles (Figure 3c). We conclude that our conducting yarns are sufficiently resilient for common textile processing, e.g., knitting, weaving, and sewing. We further studied the long-term stability of our yarns by repeating the measurements of electrical resistance on individual samples, after storage under ambient conditions. The electrical resistance increases slowly, and after 460 days storage, we measure a resistance $R = 1.5 \times R_0$ for the yarn coated once (Figure 4a). The hygroscopic nature of PSS results in absorption of water, which has been argued to cause a gradual decrease in the electrical conductivity of PEDOT:PSS films.[46−49] Kim et al. proposed that the stability at ambient conditions could be improved by removing PSS through solvent post-treatment of PEDOT:PSS films.[46]

For everyday use, e-textiles will need to sustain household laundering. This poses a challenge with PEDOT:PSS systems since the polyelectrolyte PSS is water-soluble. Interestingly, the addition of EG to PEDOT:PSS has been found to not only enhance the electrical properties but also to render the solidified blend hydrophobic.[50] We demonstrate this by a simple experiment where a yarn, which was dip-coated with unmodified PEDOT:PSS aqueous dispersion, and then stored for one year, lost its coating in a matter of minutes when submerged into water (Figure 4b, left), whereas a yarn coated with the PEDOT:PSS + EG ink is completely stable in water (Figure 4b, right). To put the yarns to the harsher test of domestic laundry, we stitched them onto standardized multifiber wash test swatches (Figures S8 and S9) and washed them up to 10 times in a household machine using a common detergent and the wool program (30 °C, spin at 800 rpm). Visual inspection did not reveal any staining on the multifiber swatches. We could however identify some losses of coating from the yarns after 10 washing cycles (Figures S8 and S9). For the twice-coated yarn,

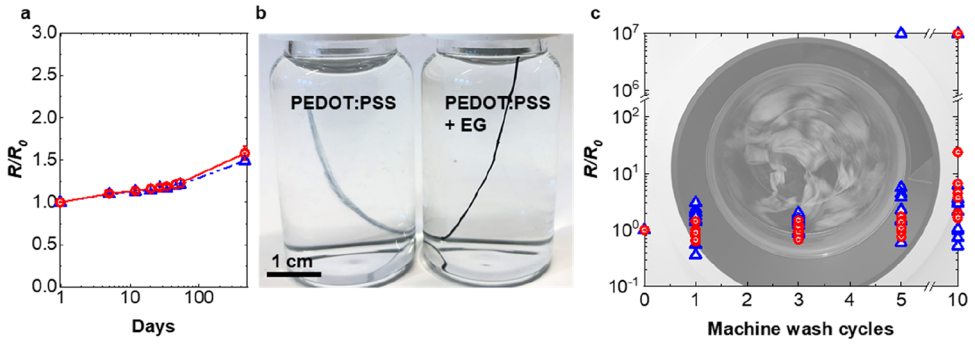


Figure 4. (a) Ratio of electrical resistance (R) measured after up to 46 days of storage under ambient conditions, divided by the initial electrical resistance (R_0) of conducting cellulose yarns coated with one (blue open triangle) or two (red open circle) coating layers. (b) Photograph of pieces of cellulose yarn coated with PEDOT:PSS and PEDOT:PSS+EG, respectively, submerged in water for several minutes. (c) R/R_0 of cellulose yarns with one (blue open triangle) or two (red open circle) coating layers after up to 10 machine wash cycles. The outlier datapoints with a value of 10^7 correspond to segments whose resistance was too high to be measured.

https://dx.doi.org/10.1021/acsami.0c15399
ACS Appl. Mater. Interfaces 2020, 12, 56403−56412

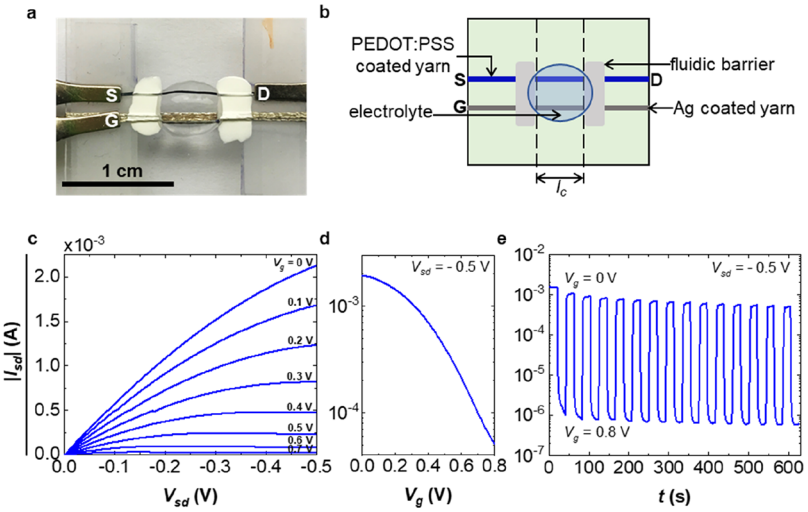


Figure 5. (a) Photograph of a yarn-based OECT illustrating the source (S), drain (D), and gate (G). The OECT was placed on a plastic slide, and nail varnish (white) was applied as a fluid barrier to control the channel length (l_c = 5 mm) prior to the application of phosphate-buffered saline. (b) Schematic of the OECT. (c) Output characteristics of a representative OECT showing the source-drain current (I_{sd}) with the corresponding source-drain voltage (V_{sd}) as the gate voltage (V_g) is increased from 0 to 0.7 V (hold time of 30 s between each sweep). (d) Transfer characteristics showing I_{sd}, while V_g was swept between 0 and 0.8 V (V_{sd} was fixed at −0.5 V). (e) I_{sd} during repeated switching of V_g between 0 and 0.8 V with a fixed V_{sd} = −0.5 V and one complete cycle being 40 s.

the resistance did not markedly change during the first five washing cycles, while the once coated yarn was able to withstand only three washing cycles (Figure 4c). More extensive washing resulted in some yarn sections that displayed a considerably higher resistance, which we explain with the partial removal of the coating.

To investigate the electrochemical functionality of our conducting cellulose yarns, we prepared and characterized e-textile OECT devices. The conducting cellulose yarn with one coating layer of PEDOT:PSS was used as a source-drain electrode, and the gate was constituted by a commercial silver-coated polyester yarn (Figure 5a,b). To study the output characteristics of our textile OECT, a gate voltage (V_g) of 0−0.7 V was applied, while a source-drain voltage (V_{sd}) sweep of 0 to −0.5 V was applied, and the corresponding source-drain current (I_{sd}) was recorded (Figure 5c). The I−V characteristics demonstrate that the channel conductivity decreases with increasing V_g, as indicated by the decrease in source-drain current (Figure 5d), i.e., the conducting coating is de-doped by the applied gate voltage enabling us to electrochemically switch off the OECT. For cyclic measurements, V_g was varied repeatedly between 0 and 0.8 V with a constant V_{sd} = −0.5 V (Figure 5e). The PEDOT:PSS yarn-based device could be switched for several cycles with an ON/OFF ratio of 10^3, which is higher than ON/OFF ratios reported for other OECTs constructed with PEDOT-based conducting fibers[51,52] and comparable to values reported for 3D-printed devices.[53] The switching speed of the here presented devices is on the order of 10 s, which could be improved by reducing the thickness of the yarn coating. These results prove two important facts as follows: (1) that the unique electrochemical properties of PEDOT are retained in the coated cellulose yarns, and (2) that the majority of the surface of the PEDOT in the yarn can be spontaneously wetted to allow liquid contact and enable electrochemistry on the entire surface of the yarn. The possibility to use these yarns in OECTs opens up the possibility to integrate more advanced wearable electronics and sensors in textiles.

A promising application for e-textiles is wearable energy scavenging, enabling conversion of biomechanical movements,[54] friction,[55] or body heat to electrical energy.[25,56] PEDOT:PSS-based textiles have been reported to function as thermoelectric generators where, owing to the Seebeck effect, a material subjected to a temperature gradient ΔT develops an electrical potential difference ΔV according to: $\Delta V = \Delta T \times \alpha$, where α is the material's Seebeck coefficient. For conductors with p-type (hole) majority charge carriers, the Seebeck coefficient is positive, and for conductors with n-type (electron) majority charge carriers, the Seebeck coefficient is negative. A thermoelectric generator consists of a number ($N_{element}$) of thermocouples, each having two "legs" made from (ideally) a p-type and an n-type material, respectively. The thermocouples are connected electrically in series and thermally in parallel to form a thermopile, and its open-circuit thermovoltage V will be given by

$$V = N_{element}(\alpha_p - \alpha_n)\Delta T \quad (2)$$

The thermopile's maximum generated power P_{max} is obtained at impedance matching conditions, i.e., when the internal resistance R_{int} is equal to the load resistance R_{load}, and can be predicted by eq 3

$$P_{max} = \frac{V^2}{4R_{int}} \quad (3)$$

PEDOT:PSS typically displays a $\alpha_p \approx 10-20\ \mu VK^{-1}$,[57−60] and for our two-layer-coated yarns, we measure α_p = 14.6 μVK^{-1}. At present, air-stable polymer n-type materials are not available, so we opted to use a commercially available silver-plated embroidery yarn, with α = 0.3 μVK^{-1} and σ_b = (1250 ± 70) Scm^{-1}. Textile thermoelectric devices have previously been constructed (Table S3) by hand-embroidery,[25] stencil/transfer printing,[61] and by vapor printing.[55] As the voltage generated by a thermopile is directly proportional to the included number of thermocouples, a textile manufacturing method suitable to produce a textile thermopile with a large number of legs, requiring a minimum of manual work, should be selected. Encouraged by the electromechanical stability of our yarns, we

https://dx.doi.org/10.1021/acsami.0c15399
ACS Appl. Mater. Interfaces 2020, 12, 56403−56412

transferred them onto a bobbin for machine sewing (Figure 6a,b) and produced a textile thermoelectric generator with the aid of a household sewing machine. The two different conducting yarns were separately stitched through three layers of felted wool fabric to form 40 out-of-plane thermocouples (Figure 6c,d). To minimize the R_{int}, we applied a commercially available textile coating containing silver particles to connect the legs in series (Figure S10) and were thus able to fabricate an energy harvesting textile using procedures common in the textile industry.

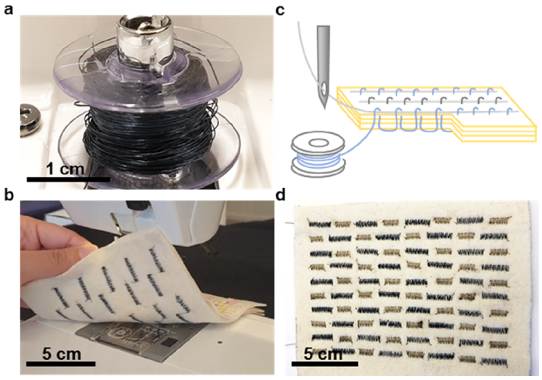


Figure 6. (a) Conducting cellulose yarn wound onto a sewing machine bobbin. (b) Machine sewing of an e-textile using the twice coated conducting cellulose yarn and a commercially available silver-plated embroidery yarn. (c) Schematic of the machine sewn stiches. The conducting yarns (blue and grey lines) were wound onto bobbins, and the sewing machine settings were adjusted to ensure that the bobbin yarn was visible on both sides of the fabric after sewing so that it penetrates the full thickness of the multilayered fabric. (d) A machine stitched all-textile thermoelectric generator with 40 out-of-plane thermocouples.

To simulate an environment that the thermoelectric textile could be utilized in, such as a cold day in the Nordic countries, we applied a temperature difference of up to ΔT = 43 °C and recorded the produced open-circuit voltage (Figure 7a). By drawing a varying current from the device, we could also measure the generated power P as a function of current I, at ΔT = 37 °C. No thermal paste or similar was applied. Notably, during practical use, there will be thermal contact resistances (c.f. Figure 7b,c) present in the system, which limit the temperature gradient effectively driving the thermopile (ΔT_{tp}) as described by

$$\Delta T_{tp} = \Delta T \times \frac{K_{tp}}{K_c + K_{tp} + K_h} \quad (4)$$

where K_{tp} is the thermal resistance of the thermopile, K_c is the contact resistance between the textile and cold reservoir, and K_h is the contact resistance between the textile and hot reservoir. Because $V_{tp}/V = \Delta T_{tp}/\Delta T$, then

$$V_{tp} = V \times \frac{K_{tp}}{K_c + K_{tp} + K_h} \quad (5)$$

The ideal open circuit voltage V was calculated (c.f. eq 2) to 21 mV (with $N_{element}$ = 40, $\alpha_{p\text{-}leg}$ = 14.6 μVK^{-1} and $\alpha_{n\text{-}leg}$ = 0.3 μVK^{-1}) at ΔT = 37 °C, and we measured a V_{tp} of 8.45 mV. From this, we could estimate the ratio of thermal contact resistance to the total thermal resistance of our thermopile $K_{tp}/K_{tot} \approx 0.4$, i.e., the ΔT_{tp} was reduced to less than half of the supplied temperature gradient ΔT. By considering K_{tp}/K_{tot}, a V_{tp} = 0.4 × V could be estimated, which was comparable to the experimental data (Figure 7a). Using this information, we could predict the maximum power output P_{max} to be 210 nW, which closely matches our experimental value of 202 nW. The performance of our textile generator favorably compares to other textile thermoelectric devices that also utilize organic materials, e.g., Elmoughni et al. reported a 32 thermocouple device, which produced P_{max} = 5 nW at ΔT = 3 K, and Ryan et al. prepared a 26 thermocouple device with P_{max} = 12 nW at $\Delta T \approx$ 66 °C.[25,61] We anticipate that thermal contact resistances will always be present in wearable systems, and that care must be taken to minimize their influence by device design optimization, e.g., by using textiles with a low thermal conductivity, and by simply making the devices thicker. Unfortunately, our household sewing machine was limited to substrate thicknesses of ~3.5 mm.

The here-presented thermoelectric textile was prepared with a stitch density of 5 passes (of thread through the fabric) per 10 mm^2, whereas an industrial embroidery machine can readily

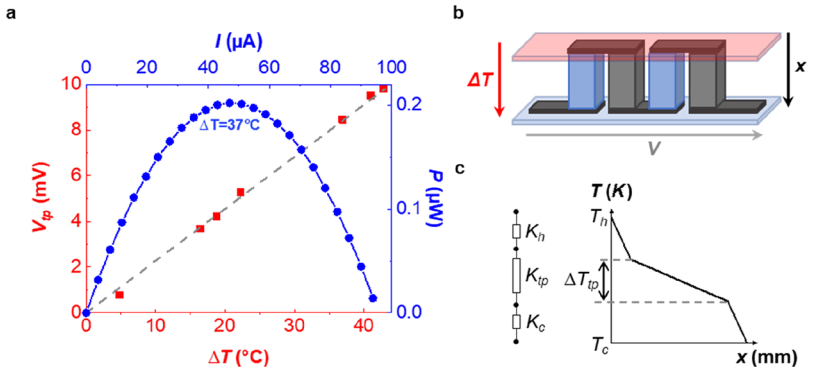


Figure 7. (a) Open-circuit voltage (V_{tp}) recorded at different temperature gradients ΔT (red squares), predicted $V_{tp} = 0.4 \times V$ (grey dashed line), and generated power P (blue filled circles+line) as a function of load current (I), for the all-textile thermoelectric generator. (b) Schematic illustration of two thermocouples of height x, the blue leg represents the conducting cellulose yarn and the grey leg is the commercially available silver-plated embroidery yarn, connected electrically in series and thermally in parallel. The light blue and light red volumes represent the thermal contact resistances on the hot and cold sides. (c) Thermal circuit representing the thermopile: the thermal resistance of the thermopile (K_{tp}) is connected in series to the thermal contact resistances between the textile surfaces and heat source (K_h) and the cold reservoir (K_c), respectively. The thermal contact resistances result in non-negligible thermal gradients (T_h and T_c) at the thermopile interfaces.

https://dx.doi.org/10.1021/acsami.0c15399
ACS Appl. Mater. Interfaces 2020, 12, 56403−56412

prepare textiles with a stitch density of 30 passes per 10 mm^2. Such an increase in stitch density would reduce the thermocouple resistance by 6 times. Moreover, an industrial machine can stitch through padded fabrics of up to 10 mm thickness, which would significantly increase the thermal resistance of the thermoelectric textile and enhance the V_{tp}. Recently, our group presented an in-depth study of the relationship between the geometry and electrical characteristics of a hand-embroidered thermoelectric textile and found that an increase in the leg length (i.e., device thickness) from 3 to 10 mm would result in a 2-fold increase in V_{tp}.[62] Consequently, by producing our device using an industrial-scale embroidery machine, we would achieve a 24 times higher output power, i.e., 4.8 μW for a device with 40 thermocouples at 37 °C. Considering the ease of scalability of our processing techniques, we expect that fabrication of a textile that produces electrical energy in the several microwatts range is feasible.

CONCLUSIONS

E-textiles maximize the utility of textile materials by adding electronic functionality to an already ubiquitous material, ideally without compromising the attractive properties of textiles such as softness, comfort, and resilience to wash-and-wear. We have presented scalable methods to coat regenerated cellulose threads and yarns, spun from an ionic liquid, with an electrically conducting ink based on PEDOT:PSS, and achieved threads with conductivities up to 36 Scm^{-1}. We further enhanced the washability of conducting yarns by adding ethylene glycol to the ink and showed that these yarns could withstand machine washing. Our cellulose yarns enable e-textile electrochemical transistors, showing potential toward woven logic circuits. Finally, we demonstrated that the mechanical durability of the threads allowed manufacturing of a 40-thermocouple fully textile thermoelectric generator by the use of a conventional sewing machine to obtain a P_{max} of 0.2 μW. With design optimization, we anticipate that a textile producing electrical energy in the microwatt range is attainable using PEDOT:PSS-coated cellulose yarns.

ASSOCIATED CONTENT

Supporting Information

The Supporting Information is available free of charge at https://pubs.acs.org/doi/10.1021/acsami.0c15399.

SEM and EDX of coated fibers, contact resistance measurements, photographs of washed samples, photograph of textile thermoelectric generator, literature survey of conducting cellulose fabrics, and textile thermoelectric generators (PDF)

AUTHOR INFORMATION

Corresponding Author

Christian Müller − *Department of Chemistry and Chemical Engineering and Wallenberg Wood Science Center, Chalmers University of Technology, 41296 Göteborg, Sweden;* orcid.org/0000-0001-7859-7909; Email: christian.muller@chalmers.se

Authors

Sozan Darabi − *Department of Chemistry and Chemical Engineering and Wallenberg Wood Science Center, Chalmers University of Technology, 41296 Göteborg, Sweden*

Michael Hummel − *Department of Bioproducts and Biosystems, Aalto University, 02150 Espoo, Finland;* orcid.org/0000-0002-6982-031X

Sami Rantasalo − *Department of Bioproducts and Biosystems, Aalto University, 02150 Espoo, Finland*

Marja Rissanen − *Department of Bioproducts and Biosystems, Aalto University, 02150 Espoo, Finland*

Ingrid Öberg Månsson − *Department of Fibre and Polymer Technology, KTH Royal Institute of Technology, 11428 Stockholm, Sweden*

Haike Hilke − *Faculty of Textiles, Engineering and Business, University of Borås, 501 90 Borås, Sweden*

Byungil Hwang − *School of Integrative Engineering, Chung-Ang University, 06974 Seoul, Republic of Korea;* orcid.org/0000-0001-9270-9014

Mikael Skrifvars − *Faculty of Textiles, Engineering and Business, University of Borås, 501 90 Borås, Sweden;* orcid.org/0000-0002-6596-8069

Mahiar M. Hamedi − *Department of Fibre and Polymer Technology and Wallenberg Wood Science Center, KTH Royal Institute of Technology, 11428 Stockholm, Sweden;* orcid.org/0000-0001-9088-1064

Herbert Sixta − *Department of Bioproducts and Biosystems, Aalto University, 02150 Espoo, Finland;* orcid.org/0000-0002-9884-6885

Anja Lund − *Department of Chemistry and Chemical Engineering, Chalmers University of Technology, 41296 Göteborg, Sweden*

Complete contact information is available at: https://pubs.acs.org/10.1021/acsami.0c15399

Notes

The authors declare no competing financial interest.

ACKNOWLEDGMENTS

We gratefully acknowledge financial support from the Wallenberg Wood Science Center (WWSC), the Knut and Alice Wallenberg Foundation through a Wallenberg Academy Fellowship, and the European Research Council (ERC) under grant agreements no. 637624 and 715268. This project was in part performed at the Chalmers Materials Analysis Laboratory (CMAL). We thank Anders Mårtensson for his assistance with the SEM measurements.

REFERENCES

(1) Zoeteman, B. C. J.; Krikke, H. R.; Venselaar, J. Handling WEEE Waste Flows: On the Effectiveness of Producer Responsibility in a Globalizing World. *Int. J. Adv. Manuf. Technol.* **2010**, *47*, 415−436.

(2) Irimia-Vladu, M. "Green" Electronics: Biodegradable and Biocompatible Materials and Devices for Sustainable Future. *Chem. Soc. Rev.* **2014**, *43*, 588−610.

(3) Tan, M. J.; Owh, C.; Chee, P. L.; Kyaw, A. K. K.; Kai, D.; Loh, X. J. Biodegradable Electronics: Cornerstone for Sustainable Electronics and Transient Applications. *J. Mater. Chem. C* **2016**, *4*, 5531−5558.

(4) Irimia-Vladu, M.; Głowacki, E. D.; Voss, G.; Bauer, S.; Sariciftci, N. S. Green and Biodegradable Electronics. *Mater. Today* **2012**, *15*, 340−346.

(5) Wang, C.; Xia, K.; Zhang, Y.; Kaplan, D. L. Silk-Based Advanced Materials for Soft Electronics. *Acc. Chem. Res.* **2019**, *52*, 2916−2927.

(6) Tobjörk, D.; Österbacka, R. Paper Electronics. *Adv. Mater.* **2011**, *23*, 1935−1961.

(7) Zhang, X.; Ye, T.; Meng, X.; Tian, Z.; Pang, L.; Han, Y.; Li, H.; Lu, G.; Xiu, F.; Yu, H.-D.; Liu, J.; Huang, W. Sustainable and Transparent

Fish Gelatin Films for Flexible Electroluminescent Devices. *ACS Nano* **2020**, *14*, 3876−3884.
(8) Jeong, H.; Baek, S.; Han, S.; Jang, H.; Kim, S. H.; Lee, H. S. Novel Eco-Friendly Starch Paper for Use in Flexible, Transparent, and Disposable Organic Electronics. *Adv. Funct. Mater.* **2018**, *28*, 1704433.
(9) Björk, P.; Herland, A.; Hamedi, M.; Inganäs, O. Biomolecular Nanowires Decorated by Organic Electronic Polymers. *J. Mater. Chem.* **2010**, *20*, 2269−2276.
(10) Głowacki, E. D.; Voss, G.; Sariciftci, N. S. 25th Anniversary Article: Progress in Chemistry and Applications of Functional Indigos for Organic Electronics. *Adv. Mater.* **2013**, *25*, 6783−6800.
(11) Bonacchini, G. E.; Bossio, C.; Greco, F.; Mattoli, V.; Kim, Y.-H.; Lanzani, G.; Caironi, M. Tattoo-Paper Transfer as a Versatile Platform for All-Printed Organic Edible Electronics. *Adv. Mater.* **2018**, *30*, 1706091.
(12) Edberg, J.; Inganäs, O.; Engquist, I.; Berggren, M. Boosting the Capacity of All-Organic Paper Supercapacitors Using Wood Derivatives. *J. Mater. Chem. A* **2018**, *6*, 145−152.
(13) Nyholm, L.; Nyström, G.; Mihranyan, A.; Strömme, M. Toward Flexible Polymer and Paper-Based Energy Storage Devices. *Adv. Mater.* **2011**, *23*, 3751−3769.
(14) Pérez-Madrigal, M. M.; Edo, M. G.; Alemán, C. Powering the Future: Application of Cellulose-Based Materials for Supercapacitors. *Green Chem.* **2016**, *18*, 5930−5956.
(15) Hoeng, F.; Denneulin, A.; Bras, J. Use of Nanocellulose in Printed Electronics: A Review. *Nanoscale* **2016**, *8*, 13131−13154.
(16) Zhang, H.; Dou, C.; Pal, L.; Hubbe, M. A. Review of Electrically Conductive Composites and Films Containing Cellulosic Fibers or Nanocellulose. *BioResources* **2019**, *14*, 7494−7542.
(17) Malti, A.; Edberg, J.; Granberg, H.; Khan, Z. U.; Andreasen, J. W.; Liu, X.; Zhao, D.; Zhang, H.; Yao, Y.; Brill, J. W.; Engquist, I.; Fahlman, M.; Wågberg, L.; Crispin, X.; Berggren, M. An Organic Mixed Ion-Electron Conductor for Power Electronics. *Adv. Sci.* **2016**, *3*, 1500305.
(18) Abol-Fotouh, D.; Dörling, B.; Zapata-Arteaga, O.; Rodríguez-Martínez, X.; Gómez, A.; Reparaz, J. S.; Laromaine, A.; Roig, A.; Campoy-Quiles, M. Farming Thermoelectric Paper. *Energy Environ. Sci.* **2019**, *12*, 716−726.
(19) Lin, Y.; Gritsenko, D.; Liu, Q.; Lu, X.; Xu, J. Recent Advancements in Functionalized Paper-Based Electronics. *ACS Appl. Mater. Interfaces* **2016**, *8*, 20501−20515.
(20) Agate, S.; Joyce, M.; Lucia, L.; Pal, L. Cellulose and Nanocellulose-Based Flexible-Hybrid Printed Electronics and Conductive Composites - A Review. *Carbohydr. Polym.* **2018**, *198*, 249−260.
(21) Lund, A.; van der Velden, N. M.; Persson, N.-K.; Hamedi, M. M.; Müller, C. Electrically Conducting Fibres for E-Textiles: An Open Playground for Conjugated Polymers and Carbon Nanomaterials. *Mater. Sci. Eng., R* **2018**, *126*, 1−29.
(22) Rahatekar, S. S.; Rasheed, A.; Jain, R.; Zammarano, M.; Koziol, K. K.; Windle, A. H.; Gilman, J. W.; Kumar, S. Solution Spinning of Cellulose Carbon Nanotube Composites Using Room Temperature Ionic Liquids. *Polymer* **2009**, *50*, 4577−4583.
(23) Hansen, S. F.; Lennquist, A. Carbon Nanotubes Added to the SIN List as a Nanomaterial of Very High Concern. *Nat. Nanotechnol.* **2020**, *15*, 3−4.
(24) *ChemSec SIN List.* https://sinsearch.chemsec.org/chemical/308068-56-6 (accessed 2020-08-25).
(25) Ryan, J. D.; Mengistie, D. A.; Gabrielsson, R.; Lund, A.; Müller, C. Machine-Washable PEDOT:PSS Dyed Silk Yarns for Electronic Textiles. *ACS Appl. Mater. Interfaces* **2017**, *9*, 9045−9050.
(26) Bashir, T.; Skrifvars, M.; Persson, N.-K. Production of Highly Conductive Textile Viscose Yarns by Chemical Vapor Deposition Technique: A Route to Continuous Process. *Polym. Adv. Technol.* **2011**, *22*, 2214−2221.
(27) Yun, Y. J.; Lee, H. J.; Son, T. H.; Son, H.; Jun, Y. Mercerization to Enhance Flexibility and Electromechanical Stability of Reduced Graphene Oxide Cotton Yarns. *Compos. Sci. Technol.* **2019**, *184*, 107845.
(28) Lima, R. M. A. P.; Alcaraz-Espinoza, J. J.; da Silva, F. A. G., Jr.; de Oliveira, H. P. Multifunctional Wearable Electronic Textiles Using Cotton Fibers with Polypyrrole and Carbon Nanotubes. *ACS Appl. Mater. Interfaces* **2018**, *10*, 13783−13795.
(29) Härdelin, L.; Hagström, B. Wet Spun Fibers from Solutions of Cellulose in an Ionic Liquid with Suspended Carbon Nanoparticles. *J. Appl. Polym. Sci.* **2015**, *132*, 41417.
(30) Zhu, C.; Chen, J.; Koziol, K. K.; Gilman, J. W.; Trulove, P. C.; Rahatekar, S. S. Effect of Fibre Spinning Conditions on the Electrical Properties of Cellulose and Carbon Nanotube Composite Fibres Spun Using Ionic Liquid as a Benign Solvent. *eXPRESS Polym. Lett.* **2014**, *8*, 154−163.
(31) Qi, H.; Schulz, B.; Vad, T.; Liu, J.; Mäder, E.; Seide, G.; Gries, T. Novel Carbon Nanotube/Cellulose Composite Fibers As Multifunctional Materials. *ACS Appl. Mater. Interfaces* **2015**, *7*, 22404−22412.
(32) Lu, J.; Zhang, H.; Jian, Y.; Shao, H.; Hu, X. Properties and Structure of MWNTs/Cellulose Composite Fibers Prepared by Lyocell Process. *J. Appl. Polym. Sci.* **2012**, *123*, 956−961.
(33) Zhang, H.; Wang, Z. G.; Zhang, Z. N.; Wu, J.; Zhang, J.; He, J. S. Regenerated-Cellulose/Multiwalled- Carbon-Nanotube Composite Fibers with Enhanced Mechanical Properties Prepared with the Ionic Liquid 1-Allyl-3-methylimidazolium Chloride. *Adv. Mater.* **2007**, *19*, 698−704.
(34) Ding, Y.; Invernale, M. A.; Sotzing, G. A. Conductivity Trends of PEDOT-PSS Impregnated Fabric and the Effect of Conductivity on Electrochromic Textile. *ACS Appl. Mater. Interfaces* **2010**, *2*, 1588−1593.
(35) Lund, A.; Darabi, S.; Hultmark, S.; Ryan, J. D.; Andersson, B.; Ström, A.; Müller, C. Roll-to-Roll Dyed Conducting Silk Yarns: A Versatile Material for E-Textile Devices. *Adv. Mater. Technol.* **2018**, *3*, 1800251.
(36) Bevilacqua, M.; Ciarapica, F. E.; Mazzuto, G.; Paciarotti, C. Environmental Analysis of a Cotton Yarn Supply Chain. *J. Cleaner Prod.* **2014**, *82*, 154−165.
(37) FAO *Building a Common Vision for Sustainable Food and Agriculture. Principles and Approaches*; ISBN 978−92−5-108471-7; Food and Agriculture Organization of the United Nations: Rome, 2014.
(38) Liebert, T. Cellulose Solvents − Remarkable History, Bright Future. In *Cellulose Solvents: For Analysis, Shaping and Chemical Modification*; American Chemical Society: 2010; Vol. *1033*, pp. 3−54.
(39) Fink, H.-P.; Weigel, P.; Purz, H. J.; Ganster, J. Structure Formation of Regenerated Cellulose Materials from NMMO-Solutions. *Prog. Polym. Sci.* **2001**, *26*, 1473−1524.
(40) Sixta, H.; Michud, A.; Hauru, L.; Asaadi, S.; Ma, Y.; King, A. W. T.; Kilpeläinen, I.; Hummel, M. Ioncell-F: A High-Strength Regenerated Cellulose Fibre. *Nord. Pulp Pap. Res. J.* **2015**, *30*, 43−57.
(41) Hummel, M.; Michud, A.; Tanttu, M.; Asaadi, S.; Ma, Y.; Hauru, L. K. J.; Parviainen, A.; King, A. W. T.; Kilpeläinen, I.; Sixta, H. Ionic Liquids for the Production of Man-Made Cellulosic Fibers: Opportunities and Challenges. In *Cellulose Chemistry and Properties: Fibers, Nanocelluloses and Advanced Materials*; Rojas, O. J., Ed.; Springer International Publishing: Cham, 2016; Vol. *271*, pp. 133−168.
(42) Asaadi, S.; Hummel, M.; Ahvenainen, P.; Gubitosi, M.; Olsson, U.; Sixta, H. Structural Analysis of Ioncell-F Fibres from Birch Wood. *Carbohydr. Polym.* **2018**, *181*, 893−901.
(43) Hwang, B.; Lund, A.; Tian, Y.; Darabi, S.; Müller, C. Machine-Washable Conductive Silk Yarns with a Composite Coating of Ag Nanowires and PEDOT:PSS. *ACS Appl. Mater. Interfaces* **2020**, *12*, 27537−27544.
(44) Whitesides, G. M. The Frugal Way: The Promise of Cost-Conscious Science. *The World in 2012* **2011**, 154.
(45) Shi, H.; Liu, C.; Jiang, Q.; Xu, J. Effective Approaches to Improve the Electrical Conductivity of PEDOT:PSS: A Review. *Adv. Electron. Mater.* **2015**, *1*, 1500017.
(46) Kim, Y. H.; Sachse, C.; Machala, M. L.; May, C.; Müller-Meskamp, L.; Leo, K. Highly Conductive PEDOT:PSS Electrode with Optimized Solvent and Thermal Post-Treatment for ITO-Free Organic Solar Cells. *Adv. Funct. Mater.* **2011**, *21*, 1076−1081.

https://dx.doi.org/10.1021/acsami.0c15399
ACS Appl. Mater. Interfaces 2020, 12, 56403−56412

(47) Alemu Mengistie, D.; Wang, P.-C.; Chu, C.-W. Effect of Molecular Weight of Additives on the Conductivity of PEDOT:PSS and Efficiency for ITO-free Organic Solar Cells. *J. Mater. Chem. C* **2013**, *1*, 9907−9915.
(48) Alemu, D.; Wei, H.-Y.; Ho, K.-C.; Chu, C.-W. Highly Conductive PEDOT:PSS Electrode by Simple Film Treatment with Methanol for ITO-free Polymer Solar Cells. *Energy Environ. Sci.* **2012**, *5*, 9662−9671.
(49) Nardes, A. M.; Kemerink, M.; de Kok, M. M.; Vinken, E.; Maturova, K.; Janssen, R. A. J. Conductivity, Work Function, and Environmental Stability of PEDOT:PSS Thin Films Treated with Sorbitol. *Org. Electron.* **2008**, *9*, 727−734.
(50) Massonnet, N.; Carella, A.; Jaudouin, O.; Rannou, P.; Laval, G.; Celle, C.; Simonato, J.-P. Improvement of the Seebeck Coefficient of PEDOT:PSS by Chemical Reduction Combined with a Novel Method for Its Transfer Using Free-Standing Thin Films. *J. Mater. Chem. C* **2014**, *2*, 1278−1283.
(51) Hofmann, A. I.; Östergren, I.; Kim, Y.; Fauth, S.; Craighero, M.; Yoon, M.-H.; Lund, A.; Müller, C. All-Polymer Conducting Fibers and 3D Prints via Melt Processing and Templated Polymerization. *ACS Appl. Mater. Interfaces* **2020**, *12*, 8713−8721.
(52) Müller, C.; Hamedi, M.; Karlsson, R.; Jansson, R.; Marcilla, R.; Hedhammar, M.; Inganäs, O. Woven Electrochemical Transistors on Silk Fibers. *Adv. Mater.* **2011**, *23*, 898−901.
(53) Bertana, V.; Scordo, G.; Parmeggiani, M.; Scaltrito, L.; Ferrero, S.; Gomez, M. G.; Cocuzza, M.; Vurro, D.; D'Angelo, P.; Iannotta, S.; Pirri, C. F.; Marasso, S. L. Rapid Prototyping of 3D Organic Electrochemical Transistors by Composite Photocurable Resin. *Sci. Rep.* **2020**, *10*, 13335.
(54) Lund, A.; Rundqvist, K.; Nilsson, E.; Yu, L.; Hagström, B.; Müller, C. Energy Harvesting Textiles for a Rainy Day: Woven Piezoelectrics Based on Melt-Spun PVDF Microfibres with a Conducting Core. *npj Flexible Electron.* **2018**, *2*, 1−9.
(55) Allison, L. K.; Andrew, T. L. A Wearable All-Fabric Thermoelectric Generator. *Adv. Mater. Technol.* **2019**, *4*, 1800615.
(56) Ryan, J. D.; Lund, A.; Hofmann, A. I.; Kroon, R.; Sarabia-Riquelme, R.; Weisenberger, M. C.; Müller, C. All-Organic Textile Thermoelectrics with Carbon-Nanotube-Coated n-Type Yarns. *ACS Appl. Energy Mater.* **2018**, *1*, 2934−2941.
(57) Zhang, L.; Deng, H.; Liu, S.; Zhang, Q.; Chen, F.; Fu, Q. Enhanced Thermoelectric Properties of PEDOT:PSS Films via a Novel Two-Step Treatment. *RSC Adv.* **2015**, *5*, 105592−105599.
(58) Myint, M. T. Z.; Hada, M.; Inoue, H.; Marui, T.; Nishikawa, T.; Nishina, Y.; Ichimura, S.; Umeno, M.; Ko Kyaw, A. K.; Hayashi, Y. Simultaneous Improvement in Electrical Conductivity and Seebeck Coefficient of PEDOT:PSS by N_2 Pressure-Induced Nitric Acid Treatment. *RSC Adv.* **2018**, *8*, 36563−36570.
(59) Luo, J.; Billep, D.; Blaudeck, T.; Sheremet, E.; Rodriguez, R. D.; Zahn, D. R. T.; Toader, M.; Hietschold, M.; Otto, T.; Gessner, T. Chemical Post-Treatment and Thermoelectric Properties of Poly(3,4-ethylenedioxylthiophene):poly(styrenesulfonate) Thin Films. *J. Appl. Phys.* **2014**, *115*, 054908.
(60) Liu, S.; Deng, H.; Zhao, Y.; Ren, S.; Fu, Q. The Optimization of Thermoelectric Properties in a PEDOT:PSS Thin Film Through Post-Treatment. *RSC Adv.* **2015**, *5*, 1910−1917.
(61) Elmoughni, H. M.; Menon, A. K.; Wolfe, R. M. W.; Yee, S. K. A Textile-Integrated Polymer Thermoelectric Generator for Body Heat Harvesting. *Adv. Mater. Technol.* **2019**, *4*, 1800708.
(62) Lund, A.; Tian, Y.; Darabi, S.; Müller, C. A Polymer-Based Textile Thermoelectric Generator for Wearable Energy Harvesting. *J. Power Sources* **2020**, *480*, 228836.

https://dx.doi.org/10.1021/acsami.0c15399
ACS Appl. Mater. Interfaces 2020, 12, 56403−56412